Frequency-Switchable Routing Protocol for Dynamic Magnetic Induction-Based Wireless Underground Sensor Networks

Guanghua Liu, *Member, IEEE*

***Abstract*—A frequency-switch strategy is introduced into the magnetic induction-based wireless underground sensor network (MI-WUSN) for its high connectivity and network throughput, which then makes routing design more complex and challenging. To this end, we study the frequency-switchable routing design to start a discussion about the high-reliability routing design of MI-WUSN. First, we analyze the frequency-selective property and map the dynamic MI-WUSN into a multilayer network. Then, we take the network throughput and energy consumption into account and formulate the frequency switchable routing decision problem in dynamic MI-WUSN as a constrained optimization problem. Finally, we evaluate how various design parameters of our obtained protocol are affecting the network performance and explore the performance limit.**

***Index Terms*—Frequency-switchable, magnetic induction (MI), routing, wireless underground sensor network (WUSN).**

I. Introduction

WIRELESS underground sensor network (WUSN) facilitates real-time monitoring and control of various underground environments with wireless sensors deployed [1], [2]. Despite promising capabilities, WUSN suffers from a significant reliability problem [3], [4]. An additional 60 dB path loss, introduced by the underground wireless channel of WUSN, makes data collection more energy-intensive and unreliable [5]. Thus, the magnetic induction (MI)-assisted wireless powered underground sensor network (MI-WPUSN), an improved WUSN, is proposed to integrate the advantages of MI communication techniques with those of wireless power transfer mechanisms [6]. The integration empowers MI-WPUSN significant potential for high reliability and energy efficiency, which are constrained by its complex and challenging data collection. To unlock the potential of MI-WPUSN, many issues are required to be resolved urgently, spreading from sensor deployment to multiple channel access control and to sensing routing establishment [6]. Herein, we focus on the sensing routing establishment for MI-WPUSN where only the underground-to-underground wireless channel constructed by MI is included, namely, so-called MI-WUSN.

Some related works have considered these routing problems for MI-WUSN [7], [8], [9], [10], [11], [12]. As an attempt to design the routing of MI-WUSN, Lin et al. [7] studied a distributed environment-aware cross-layer protocol to achieve higher throughput, and reduce energy consumption. The authors in [8] and [9] explore an energy-efficient routing protocol based on game theory for wireless sensor networks. Considering the dynamic change of the soil medium, Guo and Ben [10] derived the optimal transmission policies for underground sensors to efficiently use their energy and improve transmission reliability. Besides, Guo and Sun [11] proposed a full-duplex meta-material-enabled MI-based communication to reduce the transmission delay for multihop MI-WUSN. Digital transmission schemes for both direct and multihop MI-WUSN links were introduced in [13]. Furthermore, an adaptive transmission policy for underground sensors was explored in [12].

Despite extensive efforts on the routing problems for MI-WUSN, most of the existing works did not consider the influence of frequency-selective property [14]. In fact, MI-constructed channels have a frequency-selective property depending on the underground environment. This property makes the MI-WUSN appear to have entirely different topological structures at diverse operating frequencies [6]. Therefore, a single frequency is almost impossible to ensure that all underground sensors in MI-WUSNs are both connected and reliable. To this end, we introduce a frequency-switch strategy into each node of MI-WUSN in the routing-design phase. That is, we allow each transmitted sensor in MI-WUSN to switch its operating frequency based on related environment information when selecting the next forwarding node. Obviously, the frequency-switch strategy can significantly improve MI-WUSN connectivity and reliability by integrating all topological structures from diverse operating frequencies.

In this article, we study the frequency-switchable routing design to start a discussion about the high-reliability routing design of MI-WUSN. We consider a different-setup MI-WUSN where each sensor is in charge of both the forward selection and the corresponding operating-frequency switching of the data

Manuscript received 12 August 2023; revised 22 November 2023; accepted 19 January 2024. Date of publication 23 January 2024; date of current version 27 February 2024. This work was supported by the National Natural Science Foundation of China under Grant 62371200 and Grant 62001177. Recommended by Lead Guest Editor Hossein Fotouhi and Guest Editor Reza Malekian.

The author is with the Research Center of 6G Mobile Communications and School of Cyber Science and Engineering, Huazhong University of Science and Technology, Wuhan 430074, China (e-mail: guanghualiu@hust.edu.cn).

Digital Object Identifier 10.1109/JSAS.2024.3357792

forwarding. First, we analyze the influence of the frequency-selective property on MI-WUSN topological structures and propose our multilayer model. Then, we formulate and simplify the frequency-switchable routing decision problem in dynamic MI-WUSN, and explore its performance limit. Finally, we evaluate how various design parameters of our obtained protocol are affecting the network performance.

II. System Model

A. Frequency-Selective Link Model

This frequency-selective property makes us have to explore a new model to describe the MI-constructed link in MI-WUSN [15]. The reason is summarized as follows. Usually, underground environments, especially in seismic region, not only consist of nonconductive soil (or concrete) and air medium, but also have other conductivity objects, such as rebars, buried metal furniture, and biological tissues [16]. Because these objects have high conductivity, eddy currents are induced on them so that the MI channel is influenced by these eddy-current-induced magnetic fields.

Let us assume the reflective objects are sorted from near to far from the transmitter coil, recorded as $1, 2, \ldots p$, and the refractive objects are sorted in the same way, recorded as $p+1, p+2, \ldots p+q$. $Z_{\mathrm{m},1}, \ldots, Z_{\mathrm{m,p}}$ are the impedances of the reflective objects and $Z_{\mathrm{m,p+1}}, \ldots, Z_{\mathrm{m,p+q}}$ are the impedances of refractive objects. $I_{\mathrm{m,i}}$ denotes the current on the ith object. $M_{\mathrm{t,i}}$ is the mutual inductance of the ith object and the transmitter coil, and $M_{\mathrm{r,i}}$ is the mutual inductance of the ith object and the receiver coil. By referring to [17], we further formulate the received voltage for the multiple mixed channel

$$\begin{cases} Z_{\mathrm{t}} I_{\mathrm{t}} - \sum\limits_{i=1}^{p} j\omega M_{\mathrm{t,i}} I_{\mathrm{m,i}} - \sum\limits_{i=p+1}^{p+q} j\omega M'_{\mathrm{t,i}} I_{\mathrm{m,i}} - j\omega M' I_{\mathrm{r}} = U_{\mathrm{s}} \\ Z_{\mathrm{r}} I_{\mathrm{r}} - \sum\limits_{i=1}^{p} j\omega M_{\mathrm{r,i}} I_{\mathrm{m,i}} + \sum\limits_{i=p+1}^{p+q} j\omega M'_{\mathrm{r,i}} I_{\mathrm{m,i}} - j\omega M' I_{\mathrm{t}} = 0 \\ Z_{\mathrm{m},1} I_{\mathrm{m},1} - j\omega M_{\mathrm{t},1} I_{\mathrm{t}} - j\omega M_{\mathrm{r},1} I_{\mathrm{r}} = 0 \\ \vdots \\ Z_{\mathrm{m,p}} I_{\mathrm{m,p}} - j\omega M_{\mathrm{t,p}} I_{\mathrm{t}} - j\omega M_{\mathrm{r,p}} I_{\mathrm{r}} = 0 \\ Z_{\mathrm{m,(p+1)}} I_{\mathrm{m,(p+1)}} - j\omega M'_{\mathrm{t,(p+1)}} I_{\mathrm{t}} + j\omega M'_{\mathrm{r,(p+1)}} I_{\mathrm{r}} = 0 \\ \vdots \\ Z_{\mathrm{m,(p+q)}} I_{\mathrm{m,(p+q)}} - j\omega M'_{\mathrm{t,(p+q)}} I_{\mathrm{t}} + j\omega M_{\mathrm{r,(p+q)}} I_{\mathrm{r}} = 0. \end{cases} \tag{1}$$

By solving the equations, we obtain the received current and power as the following:

$$I_r = \frac{\sum\limits_{i=1}^{p} j\omega M_{\mathrm{r,i}} I_{\mathrm{m,i}} - \sum\limits_{i=p+1}^{p+q} j\omega M'_{\mathrm{r,i}} I_{\mathrm{m,i}} + j\omega M' I_{\mathrm{t}}}{Z_{\mathrm{r}}} \tag{2}$$

$$P_r = \frac{1}{2} |I_{\mathrm{r}}|^2 R_{\mathrm{L}}. \tag{3}$$

From (2) and (3), both the number and order of reflective and refractive objects greatly affect the received power, which depends on underground environment. Furthermore, at same underground location, the operating frequency ω becomes the main force in changing receiving power. Therefore, for each MI channel, the signal strength at MI receiver will be distinctly different when the MI transmitter sends its data with diverse operating frequencies. To this end, for a given communication distance, we replace P_r with P_r^{ij} to represent the received signal strength at MI receiver indexed by j. It could be denoted by the function of the operating frequency ω at MI transmitter indexed by i, i.e., $P_r^{ij} = g(\omega)$. What is more, these MI channels distributed in different locations have diverse frequency-selective law, i.e., $P_r^{ij} = g_{ij}(\omega)$. Moreover, the underground environment is usually dynamic (i.e., time-varying) due to many uncertain factors (e.g., frequent aftershocks). That is, the aforementioned $g_{ij}(\cdot)$ is further portrayed as a time-varying mapping relationship denoted by $g_{ij}^t(\cdot)$. Therefore, the frequency-selective link model is

$$P_r^{ij} = g_{ij}(\omega, t). \tag{4}$$

This property makes MI-constructed links appear different feasibilities for data transmission at diverse operating frequencies and time instants. That is, unlike prior works [18], [19], in this article, MI link connectivity is no longer fixed and varying with operating frequency and time instant. Therefore, we are required to further study the network model of dynamic MI-WUSN with the influence of frequency-selective property.

B. Multilayer Network Model

An example of the dynamic MI-WUSN is shown in Fig. 1, which consists of N underground sensors and one sink. These nodes are assumed to be equipped with MI antennas, which can work with diverse operating frequency in band W. The set of these nodes is denoted as $U = \{u_0, u_1, \ldots, u_N\}$, where u_0 represents the unique sink and the remaining $u_i,\ i = 1, \ldots, N$ stand for the underground sensors. To ensure node u_j successfully receiving the transmitted data from the previous node u_i, $i, j \in D$, where $D \triangleq \{0, 1, \ldots, N\}$, the link quality meets certain requirements. Based on the aforementioned frequency-selective link model, the receiving signal power of u_j is denoted by $P_r^{ij}(\omega, t)$, and required to be not less than the receiver sensitivity P_s. Moreover, we consider the underground environment changes every Δt and then denote the set of all changing time instant as $T = \{t_0, t_1, \ldots, t_s, t_{s+1}, \ldots, t_M\}$, where $t_s - t_{s-1} = \Delta t,\ s \in N^+$ and t_M is the permissible duration. Thus, the multilayer network model is denoted as

$$\mathscr{M} = (\mathscr{G}, \mathscr{W}, \mathscr{T}) \tag{5}$$

where $\mathscr{G}$, $\mathscr{W}$, and $\mathscr{T}$ are systematically expressed as follows.

Specifically, $\mathscr{G}$ is defined as a family of weighted graphs $G_{\omega t} = (X_{\omega t}, E_{\omega t})$ (called layers of $\mathscr{M}$), namely

$$\mathscr{G} = \{G_{\omega t};\ \omega \in W,\ t \in T\}. \tag{6}$$

Therein, $E_{\omega t}$ represents the set of *intraconnections* (i.e., feasible MI channel) between diverse nodes in the layer $G_{\omega t}$. The set of nodes of the layer $G_{\omega t}$ is denoted by $X_{\omega t} = \{x_0^{\omega t}, x_1^{\omega t}, \ldots, x_N^{\omega t}\}$, where $x_i^{\omega t}$ is the label of node u_i at the layer $G_{\omega t}$ for $i \in D$. In addition,

$$\mathscr{W} = \Big\{ E_{\omega_1\omega_2} \triangleq \{(x_i^{\omega_1 t}, x_i^{\omega_2 t}); i \in D\}; \\ \omega_1, \omega_2 \in W,\ \omega_1 \neq \omega_2 \Big\} \tag{7}$$

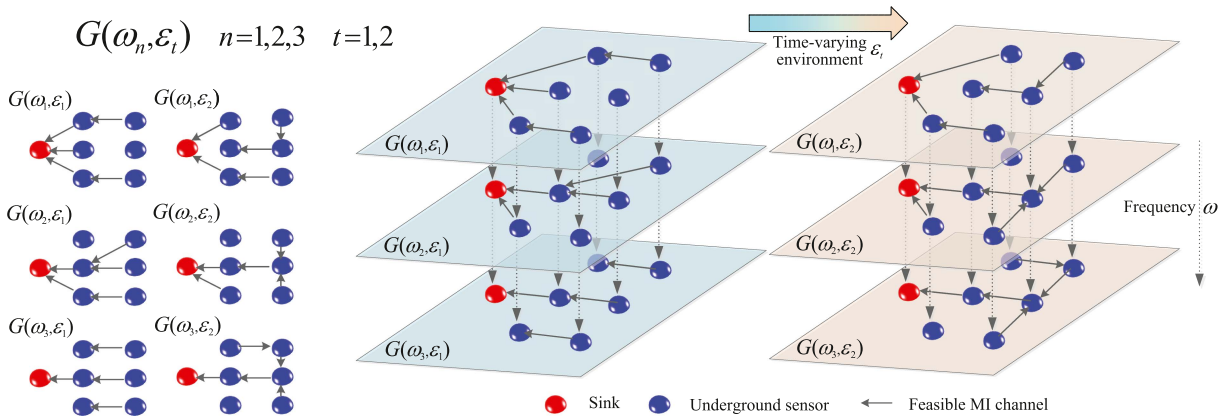

Fig. 1. Schematic illustration of the mapping of a dynamic MI-WUSN into a multilayer network. At each time instant $t = 1, 2$ (represents environment ε_t) and frequency ω_n, $n = 1, 2, 3$, the structure of interactions between the sink and underground sensors (left-hand side). The corresponding multilayer network representation where each time instant and frequency is mapped into a different layer (right-hand side).

is the set of *interconnections* between nodes at different layers $G_{\omega_1 t}$ and $G_{\omega_2 t}$ with $\omega_1 \neq \omega_2$ for $\forall\, t \in T$, and

$$\mathscr{T} = \Big\{E_{t_s t_{s+1}} \triangleq \{(x_i^{\omega t_s}, x_i^{\omega t_{s+1}}); i \in D\}; \\ t_s, t_{s+1} \in T, s \in N^+\Big\} \tag{8}$$

is the set of directed *interconnections* from nodes at the earlier layers $G_{\omega t_s}$ to that at the later $G_{\omega t_{s+1}}$ with $s \in N^+$ for $\forall\, \omega \in W$. The adjacency matrix of each layer $G_{\omega t}$, thus, can be denoted by $A^{\omega t} = [a_{ij}^{\omega t}] \in \mathbb{R}^{(N+1)\times(N+1)}$, where

$$a_{ij}^{\omega t} = \begin{cases} P_r^{ij}(\omega, t), & \text{if } P_r^{ij}(\omega, t) \geq P_s \\ 0, & \text{otherwise} \end{cases} \tag{9}$$

for $0 \leq i, j \leq N, \omega \in W$, and $t \in T$. Note that the edge weighs corresponding to $E_{\omega_1\omega_2}$ and $E_{t_s t_{s+1}}$ are set to be 1. For convenience of expressions, we apply $e_{\omega_1\omega_2}$ and $e_{t_s t_{s+1}}$ to represent the elements of $E_{\omega_1\omega_2}$ and $E_{t_s t_{s+1}}$, respectively, and $e_{ij}^{\omega t}$ ($i \neq j$ and $i, j \in D$) denote the elements of $E_{\omega t}$.

III. Frequency-Switchable Routing Design

In this section, we characterize the frequency-switchable routing decision problem based on the multilayer network model introduced in Section II under a fixed energy supply. Without loss of generality, we consider a case where a certain underground sensor node (let it be u_1) is required to transmit data to the unique sink u_0.

A. Problem Formulation

Consider our network model $\mathscr{M}$ as a directed graph $(V_{\mathscr{M}}, E_{\mathscr{M}})$ with vertex set $V_{\mathscr{M}}$ and edge set $E_{\mathscr{M}}$ by referring to [20]. In fact, a large portion of edges in $\mathscr{M}$, excepting for the interconnections in $\mathscr{T}$, is undirected. To this end, we refer to the aforesaid edge as two opposing directed edge to assure $\mathscr{M}$ a thorough directed graph. Then, we have

$$V_{\mathscr{M}} = \bigcup_{\omega\in W}\bigcup_{t\in T} X_{\omega t} \\ E_{\mathscr{M}} = \mathscr{W}^+ \cup \mathscr{T} \cup \{E_{\omega t};\ \omega \in W,\ t \in T\}^+ \tag{10}$$

where the function $(\cdot)^+$ can make the undirected edge replaced with two opposing directed edges in the set. For dynamic MI-WUSN, the routing decision problem becomes in fact to find the paths to max the flow f from *origin* vertex to *terminus* vertex in $\mathscr{M}$ under a fixed energy supply, which means the maximum transmission data amount. Note that the element in $V_{\mathscr{M}}$ actually is the layer label of N underground sensor node $\{u_1, \ldots, u_N\}$ and one sink node u_0. That is, in this article, *origin* is a set denoted by

$$V_{\text{or}} = \{x_1^{\omega t};\ \omega \in W,\ t \in T\} \tag{11}$$

and *terminus* is also a set denoted by

$$V_{\text{te}} = \{x_0^{\omega t};\ \omega \in W,\ t \in T\}. \tag{12}$$

Therefore, by referring to existing flow-network theory [21], the flow f is defined as a real-valued function on vertex pairs or edges satisfying the following constraints:

$$-c(\vec{e}) \leq f(\vec{e}) \leq c(\vec{e})\ \forall \vec{e} \in E_{\mathscr{M}} \tag{13a}$$

$$f(\vec{e}) = -f(-\vec{e})\ \forall \vec{e} \in E_{\mathscr{M}} \tag{13b}$$

$$\sum_{u\in V_{\mathscr{M}}} f(u, v) = 0\ \forall v \in V_{\mathscr{M}} - (V_{\text{or}} \cup V_{\text{te}}). \tag{13c}$$

Therein, (13a) is used to assure the flow less than the capacity $c(\cdot)$ of MI-constructed communication link. Equation (13b) eliminates the possibility of having positive flow on both two directionally opposing edges $\vec{e}$ and $-\vec{e}$. Moreover, (13b) is the flow conservation constraint.

From the above, f is the net flow into the *terminus*

$$\sum_{u\in V_{\mathscr{M}}}\sum_{v\in V_{\text{te}}} f(u, v). \tag{14}$$

Moreover, as one of the key questions in MI-WUSN, the energy consumption must be taken into account to make sure the results are realistic. To this end, we introduce expressions $E_i(f(\vec{e}))\ \forall\, i \in D$ representing the energy cost of node u_i when the data flow $f(\vec{e})$ occurs at edge $\vec{e}$. It is assumed that the initial energy of each underground sensor is E_0. Then, we formulate

the frequency-switchable routing decision problem in dynamic MI-WUSN as follows:

$$\mathcal{P}0: \max_{\{f(\vec{e})\}} \sum_{u\in V_{\mathscr{M}}}\sum_{v\in V_{\text{te}}} f(u,v) \tag{15a}$$

$$\text{s.t.} \quad \mathscr{M} \text{ is a connected graph} \tag{15b}$$

$$\vec{e} \in E_{\mathscr{M}} \tag{15c}$$

$$-c(\vec{e}) \le f(\vec{e}) \le c(\vec{e}) \tag{15d}$$

$$\sum_{\{f(\vec{e})\}} E_i(f(\vec{e})) \le E_0, \quad i=1,\dots,N. \tag{15e}$$

Obviously, (15) can be considered as a maxflow problem by referring to [20], and the optimal solution $\{f(\vec{e})\}^*$ should be a set containing the assigned optimal flow $f^*(\vec{e})$ for each edge $\vec{e}$, which can max the net data amount (derived from u_1) into u_0. Note that $\mathcal{P}0$ is a multisource multisink maxflow problem. There are usually two ways of thinking about this problem: importing virtual unique source/sink node and traversing source-sink pairs [22]. In fact, we cannot assign physical meaning to the imported virtual node in a multilayer network, so that the former scheme is useless for $\mathcal{P}0$. However, we are also powerless to deal with $\mathcal{P}0$ by an ergodic method due to the following fundamental differences.

1) The number of origin/terminus nodes in $\mathcal{P}0$ actually is equal to $(M+1)\cdot cout(W)$, where $cout(W)$ is the number of selectable frequency points in band W. Note that, the larger the M or $cout(W)$ is, the more precise $\mathscr{M}$ can describe the actual scene. That limits greatly the practicability of the ergodic method in problem $\mathcal{P}0$.
2) There are many directed edges that have no practical significance in $\mathcal{P}0$, which are produced in the replacement process for intrinsic undirected edges. The ergodic method then is difficult to meet our needs due to a lot of computation overheads in the search for these edges.

B. Solution

From the above, the main difficulty of solving is induced by multiple origin/terminus nodes of $\mathscr{M}$. In fact, these origin/terminus nodes are only the labels of real sensor node u_i, $i\in D$ at diverse operating frequencies and time instants. To this end, we try to treat the actual communication links between real sensor node as optimization variables rather than the connections between their labels.

For the actual link, each routing decision in $\mathscr{M}$ contains two phases: frequency selection and next-forwarder selection, different from the conventional routing design. Specifically, we first determine the next forwarder relying on some well-designed basis. Given the next node, we should choose the optimal operating frequency, at which the channel has the maximum frequency response, to send data packets for good transmission performance. However, the frequency selection and next-forwarder selection are carried out at the same time. That is because the selection of operating frequency determines feasible adjacent sensors and further restricts the next-forwarder selection, while the next-forwarder selection means an actual physical link and further determines the optimal operating frequency. Therefore, it is necessary to integrate these two phases into one concept, namely, *step*. In other words, *step* $u_i \to u_j$ means the node u_i choosing u_j as the next forwarder to send packets with the optimal operating frequency of the underground channel between u_i and u_j. To explain *step* more systematically, we formulate the operating frequency and next-forwarder selection with the labels in $\mathscr{M}$ as the following.

Definition 1: The *frequency selection phase* (FSP) $S_F^{\omega(i)}$ represents the process to choose a feasible operating frequency $\omega(i)$ for u_i, at which the MI channel can successfully transmit at least one packet from u_i to other sensors during Δt. With give initial operating frequency ω_0 and time instant t_0, $S_F^{\omega(i)}$ can be expressed by

$$x_i^{\omega_0 t_0} e_{\omega_0\omega(i)} x_i^{\omega(i)t_0}. \tag{16}$$

It is worth mentioning that the feasible operating frequency $\omega(i,t_0)$ (for simplicity, it is abbreviated to $\omega(i)$ when there is no ambiguity) means that $\exists\, l\in D$ such that u_l is active (e.g., with enough energy), the link $(x_i^{\omega(i)t_0}, x_l^{\omega(i)t_0}) \in E_{\omega(i)t_0}$, and the transmission rate on $(x_i^{\omega(i)t_0}, x_l^{\omega(i)t_0})$ is not less than 1 packet per Δt. For these l's $\in D$, u_l is the *neighbor* of u_i when $\omega=\omega(i)$ and time instant is t_0, whose label is $x_l^{\omega(i)t_0}$.

Definition 2: The *information transmission phase* (ITP) T_I^{ik} represents the process to choose a neighbor u_k of u_i after FSP and further transmit aforementioned packets from u_i to it during the period of Δt. When the transmission duration of two packets is less than Δt, T_I^{ik} can be given by

$$x_i^{\omega(i)t_0} e_{ik}^{\omega(i)t_0} x_k^{\omega(i)t_0}. \tag{17}$$

On the contrary, T_I^{ik} should be expressed with

$$x_i^{\omega(i)t_0} e_{ik}^{\omega(i)t_0} x_k^{\omega(i)t_0} e_{t_0t_1} x_k^{\omega(i)t_1} \tag{18}$$

which contains one intraconnection and one interconnection in $\mathscr{M}$. The intraconnection $e_{ik}^{\omega(i)t_0}$ represents the transfer of information and the interconnection $e_{t_0t_1}$ depicts the time drains.

Based on the above two definitions, a *step* in $\mathscr{M}$ can be denoted by

$$S_F^{\omega(i)} T_I^{ij} \tag{19}$$

whose terms are successively FSP and ITP, which means that at least one packet is successfully forwarded. It is worth mentioning that *step* defined in this framework cannot be considered as a hop in the conventional sense. For the sake of clarity, we say that $S_{ij}^{\omega(i)}(t_s)$ is a step in $\mathscr{M}$, by which u_i can send at least one packet to u_j from t_{s-1} to t_s with operating frequency $\omega(i)$. Further, we call the number of transferable packets in this step the *capacity* of $S_{ij}^{\omega(i)}(t_s)$, denoted by $\varepsilon(S_{ij}^{\omega(i)}(t_s))$. In addition, we apply $E_i(S_{ij}^{\omega(i)})$ and $E_j(S_{ij}^{\omega(i)})$ to, respectively, depict the energy consumption at u_i and u_j in step $S_{ij}^{\omega(i)}$.

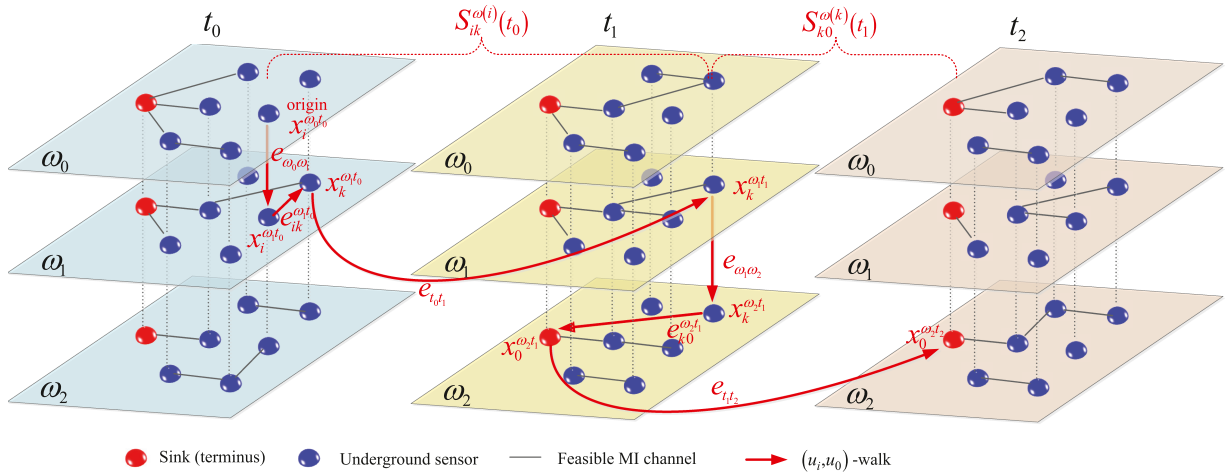

Fig. 2. Schematic of a walk (arrow trajectories) from underground sensor u_i to the sink u_0, $i \in D$ in $\mathscr{M}$. This illustration evinces how the frequency-switch strategy allows a walker (packet) to move between nodes that belong to disconnected components on a given layer.

Further, we can define a *walk* in $\mathscr{M}$ by a finite non-null step sequence

$$S_{ik_1}^{\omega(i)}(t(k_1))S_{k_1k_2}^{\omega(k_1)}(t(k_2))\dots S_{k_Rj}^{\omega(k_R)}(t(j)) \tag{20}$$

whose terms are successively steps from u_i to u_j. Therein, $t(k_r) \in T,\ r = 1,\dots,R$ satisfy the following inequality: $t(k_r) < t(j) \le t_M$. We say that $W_{ij}(t(k_1), t(j))$, abbreviated as W_{ij}, is a walk from u_i to u_j during time from $t(k_1) - \Delta t$ to $t(j)$, or a (u_i, u_j)-walk in $\mathscr{M}$. u_i and u_j are called *origin* and *terminus* of $\mathscr{M}$, respectively, and $u_{k_1}, u_{k_2}, \dots, u_{k_R}$ are its *internal/relay nodes*. Based on the above analysis, $\min\{\varepsilon(S_{ik_1}^{\omega(i)}(t(k_1))), \varepsilon(S_{k_1k_2}^{\omega(k_1)}(t(k_2))), \dots, \varepsilon(S_{k_Rj}^{\omega(k_R)}(t(j)))\}$ is considered as the *capacity* of W_{ij}, denoted by $\varepsilon(W_{ij})$. Fig. 2 illustrates a walk from $u_i,\ i \in D$ to u_0, i.e., a (u_i, u_0)-walk in $\mathscr{M}$, where there is only one internal node $u_k,\ k \in D$. Further, we give the definition of *connected* in $\mathscr{M}$, which is one of the most important concept in routing designing, as the following.

Definition 3: An underground sensor u_i is called a *connected* node in $\mathscr{M}$ if and only if it has a (u_i, u_0)-walk to the sink u_0, i.e., u_i is connected $\equiv \exists$ active $k \in D$, which has a walk $W_{ik}(t_0 + \Delta t, t(k))$ and a step $S_{k0}(t(0))$, where $t(0) > t(k),\ t(0), t(k) \in T$ and t_0 represents the starting time of the first step in walk W_{ik}.

In fact, when u_i is connected, there could exist multiple walks from u_i to u_0, which constitute a set of walks denoted by $\mathscr{D}_i$. Note that each walk in $\mathscr{D}_i$ can be decomposed into one or more steps. With a view to a finite number of steps in $\mathscr{M}$, different walks could have same steps. To this end, we propose a new concept, *utilization*, which is used to depict the number of repetitions in diverse walks from $\mathscr{D}_i$. We further say that $U(S_{k_1k_2}(t_s))$ is the utilization of the step $S_{k_1k_2}(t_s) \in \mathscr{D}_i$. To simplify the expression, for a set of walks, $|\cdot|$ is used for representing its number of different walks, respectively, and $||\cdot||$ its number of different steps in the sequel.

In this case, the best set of walks $\mathscr{B} \subset \cup_i \mathscr{D}_i$, to transmit as many packets as possible from u_1 to u_0 under a fixed energy supply, is the optimal solution to our routing decision problem $\mathcal{P}0$. Meanwhile, the original problem $\mathcal{P}0$ can be reformulated into the following:

$$\mathcal{P}1: \max_{W_{10}^k \in \mathscr{B}} \sum_{k=1}^{|\mathscr{B}|} \varepsilon(W_{10}^k) \tag{21a}$$

$$\text{s.t.} \quad u_1 \text{ is connected} \tag{21b}$$

$$\mathscr{B} \subset \mathscr{D}_1 \tag{21c}$$

$$U(S^j) \le \varepsilon(S^j), \quad j = 1,\dots,||\mathscr{B}|| \tag{21d}$$

$$\sum_{j=1}^{||\mathscr{B}||} E_i(S^j) \le E_0, \quad i = 1,\dots,N \tag{21e}$$

where $S^j \in \mathscr{B},\ j = 1,\dots,||\mathscr{B}||$.

Obviously, after many complex and tedious transformations, the considered frequency-switchable routing decision problem in dynamic MI-WUSNs becomes easier to understand and process. However, the global information of MI-WUSNs to solve the optimal problem seems to be unavailable, although there are some attempts to make it with the help of effective forecasting about underground environment [23]. In fact, the efficient distributed implementation is a valuable and necessary work but not the focus of our attention in this article. As a novel understanding about the routing design, frequency-switchable routing tries to start a discussion about the sensing routing design of dynamic MI-WUSNs with the frequency-selective property.

Subsequently, a more pressing task is to explore the performance limit of our frequency-switchable routing. To this end, we easily design a corresponding centralized solution algorithm to solve $\mathcal{P}1$ and obtain the best set of walks $\mathscr{B}$, i.e., the optimal frequency-switchable routing. The algorithm is implemented in two stages: searching and determining, which are illustrated in Algorithm 1. First, we apply the backtracking algorithm to search for all possible walks from u_1 to u_0. Then, by means of a bubblesort-like procedure, we further determine the best set of walks $\mathscr{B}$, which maximize network throughput under the energy

Algorithm 1: Frequency-Switchable Routing Algorithm.

Input: N, E_0, $W = \{\omega_0, \omega_1, \ldots, \omega_l, \omega_{l+1}, \ldots, \omega_L\}$, $T = \{t_0, t_1, \ldots, t_s, t_{s+1}, \ldots, t_M\}$;
Output: the best set of walks $\mathscr{B}$;

1) **Search for possible walks**
initialize multilayer network $\mathscr{M}$ with weight $\varepsilon(\cdot)$;
while $(t < t_M)$ **do**
Backtrack(i≤ N){
nextNodes=findPath(u_i connected to u_1/Paths in $\mathscr{M}$);
partialPaths=link(u_1/Paths, nextNodes);
if(nextNodes=u_0){partialPaths join possibleWalks $\mathscr{D}_1$;}
else{update i=i+1;}
end if}
end while
2) **Determine the best set of walks**
obtain the number of Walks $|\mathscr{D}_1|$; bestWalks $\mathscr{B}$=[];
for $j = 1, 2, \ldots, |\mathscr{D}_1|$ **do**
bestValue $\varepsilon(\mathscr{B}) = \sum_{\text{Walks}\in\mathscr{B}} \varepsilon(\text{Walks})$;
tempSet=unite($\mathscr{B}$, possibleWalks(j));
if (tempSet meets the constraints (21c) and (21d)){
$\mathscr{B}$=tempSet; $\varepsilon(\mathscr{B}) = \varepsilon(\text{tempSet})$;}
else{**for** $p = 1, 2, \ldots, |\mathscr{B}|$ **do**
repSet=replace($\mathscr{B}$(p),possibleWalks(j));
if(ε(repSet) > $\varepsilon(\mathscr{B})$ and repSet meets (21c)&(21d)){
$\mathscr{B}$=repSet; $\varepsilon(\mathscr{B}) = \varepsilon(\text{repSet})$;}
end if
end for}
end if
end for

constraint. Although it is a centralized algorithm that is difficult to be directly applied in practice, Algorithm 1 can be given as a revelation or reference.

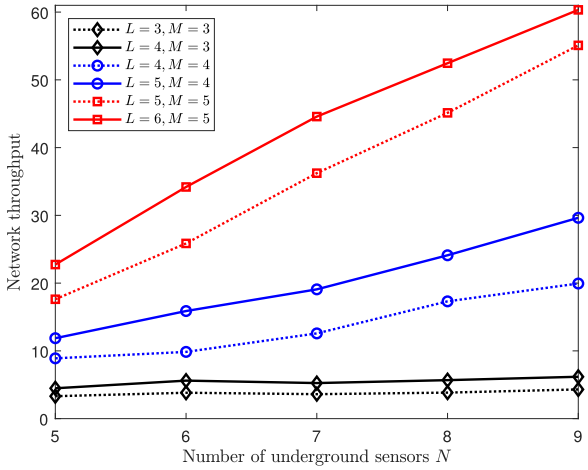

Fig. 3. Network throughput versus the number of underground sensors.

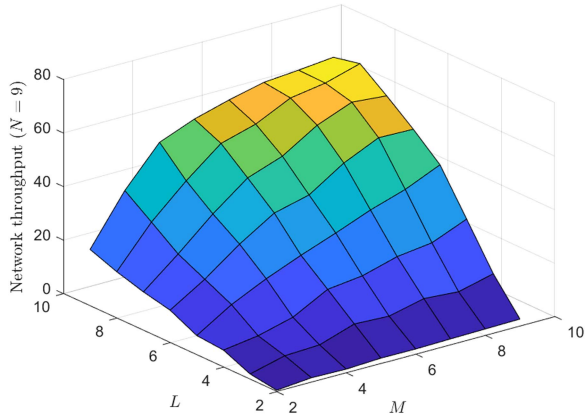

Fig. 4. Network throughput versus L and M.

IV. Performance Evaluation

In this section, numerical results are presented to explore the performance limit of the frequency-switchable routing protocol $\mathscr{B}$ in a dynamic MI-WUSN with diverse parameters. These parameters used in the simulations are the same as those used in Sections II and III. Specifically, one sink and N underground sensors are deployed in a square area with a fixed size, where one sensor node is chosen to be the origin. Further, we randomly initialize all adjacency matrices $A^{\omega_l t_s}$ for these sensor nodes, whose entries represent the number of transferable packets between two nodes with operating frequency ω_l, $l \in \{0, 1, \ldots, L\}$ from time instant t_s to t_{s+1}, $s \in \{0, 1, \ldots, M-1\}$. Moreover, to highlight the impact of routing, the residual energy E_0 of every sensor except the origin is initially set to be limited 30 and reduces 1 when the sensor forwards a packet.

Fig. 3 demonstrates the network throughput of our routing, in terms of the total number of packets successfully transmitted to the sink within permissible duration, by averaging 1000 randomly generated multilayer network. Network throughput is roughly increasing with N, as shown in Fig. 4. This observation makes sense, since more nodes can introduce more relay selections into MI-WUSN, which likely results in more walks from the origin to the sink. Meanwhile, we find that network throughput is low and its growing trend is not obvious when L or M is small. That is because small L and M mean short run duration and low-frequency-switch ability, respectively, which prevents the emergence of more feasible links. To further illustrate how these system parameters of our routing are affecting the performance, the network throughput for diverse L and M is shown in Fig. 4. It is observed that network throughput increases with L and M and gradually reaches a steady state due to the energy and bandwidth constraints, which can help us build a lower cost network.

From the above, the frequency selectivity is originating from those point-to-point channels or links, which are affected by the secondary magnetic field from the eddy of conductive objects. That is, the fluctuations in link quality can measure the impact of frequency selectivity to some extent. Given $L = 6$ and $M = 5$, we then illustrate the network throughput with varying link-quality volatility K, which is in terms of the ratio of the difference between the maximum and minimum throughputs to the maximum value, as shown in Fig. 5. Therein, the link average quality is assumed to be same. It is observed that the network throughput quickly increases with K. That is because bigger K means greater differences in link quality formed by

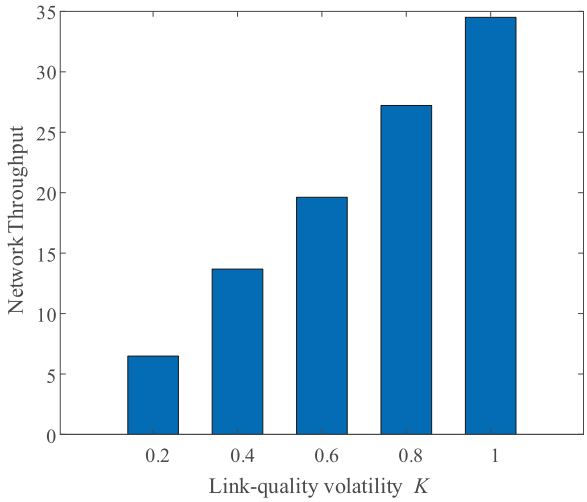

Fig. 5. Network throughput versus link-quality volatility K.

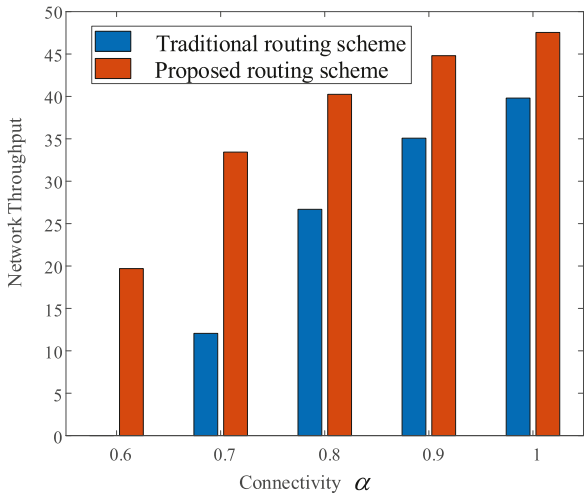

Fig. 6. Network throughput versus connectivity α.

different operating frequencies. These differences not only limit the application of traditional routing, but also provide space for our frequency-switchable routing to be applied.

Fig. 5 makes an attempt to demonstrate the impact of link quality and ignores the connectivity. In fact, the connectivity is one of the most important concepts for routing designing. To introduce the effect of frequency selectivity, the connectivity α is defined as the feasible-link ratio in a planar graph formed from the superposition of different frequency and time layers $G_{\omega t}$. Fig. 6 illustrates the trend of the network throughput of the frequency-switchable routing protocol with α. The number of sensors is set to $N = 5$, the operating frequency band to $L = 6$, and the time during to $M = 5$. It can be seen that the throughput becomes progressively larger with increasing values of α. This makes sense because the sensor node has more feasible path choices. Moreover, the performance of our frequency-switchable routing is significantly better than traditional routing where the dynamic MI-WUSN is equivalent to a single-frequency network. That is because the real connectivity of the single-frequency MI-WUSN is far below α. In a word, exploring the performance limit shows a great potential of our frequency-switchable routing protocol.

V. Conclusion

In this article, we studied the frequency-switchable routing design in the MI-WUSN to start a discussion about the sensing routing design of MI-WPUSN. Considering the frequency-selective property, we first mapped the dynamic MI-WUSN into a multilayer network. Then, based on our constructed multilayer model, we took the network throughput and energy consumption into account and formulated the frequency-switchable routing decision problem in dynamic MI-WUSN as a constrained optimization problem. Further, we adopted a centralized solution algorithm to explore the performance limit of our frequency-switchable routing design by simulations.

References

[1] I. F. Akyildiz and E. P. Stuntebeck, "Wireless underground sensor networks: Research challenges," *Ad Hoc Netw.*, vol. 4, pp. 669–686, Apr. 2006.
[2] K. Lin and T. Hao, "Link quality analysis of wireless sensor networks for underground infrastructure monitoring: A non-backfilled scenario," *IEEE Sensor J.*, vol. 21, no. 5, pp. 7006–7014, Mar. 2021.
[3] G. Liu, Z. Wang, and T. Jiang, "QoS-aware throughput maximization in wireless powered underground sensor networks," *IEEE Trans. Commun.*, vol. 64, no. 11, pp. 4776–4789, Nov. 2016.
[4] G. Liu, Z. Sun, and T. Jiang, "Joint time and energy allocation for QoS-aware throughput maximization in MIMO-based wireless powered underground sensor networks," *IEEE Trans. Commun.*, vol. 67, no. 2, pp. 1400–1412, Feb. 2019.
[5] I. F. Akyildiz, Z. Sun, and M. C. Vuran, "Signal propagation techniques for wireless underground communication networks," *Phys. Commun.*, vol. 2, no. 3, pp. 167–183, Sep. 2009.
[6] G. Liu, "Data collection in MI-assisted wireless powered underground sensor networks: Directions, recent advances, and challenges," *IEEE Commun. Mag.*, vol. 59, no. 4, pp. 132–138, Apr. 2021.
[7] S.-C. Lin, I. F. Akyildiz, P. Wang, and Z. Sun, "Distributed cross-layer protocol design for magnetic induction communication in wireless underground sensor networks," *IEEE Trans. Wireless Commun.*, vol. 14, no. 7, pp. 4006–4019, Jul. 2015.
[8] D. Lin and Q. Wang, "A game theory based energy efficient clustering routing protocol for WSNs," *Wireless Netw.*, vol. 23, no. 4, pp. 1101–1111, May 2017.
[9] D. Lin and Q. Wang, "An energy-efficient clustering algorithm combined game theory and dual-cluster-head mechanism for WSNs," *IEEE Access*, vol. 7, pp. 49894–49905, 2019.
[10] H. Guo and B. Ben, "Reinforcement learning-enabled reliable wireless sensor networks in dynamic underground environments," in *Proc. IEEE Mil. Commun. Conf.*, 2019, pp. 646–651.
[11] H. Guo and Z. Sun, "Full-duplex metamaterial-enabled magnetic induction networks in extreme environments," in *Proc. IEEE Conf. Comput. Commun.*, 2018, pp. 558–566.
[12] D. Zhao, Z. Zhou, S. Wang, B. Liu, and W. Gaaloul, "Reinforcement learning enabled efficient data gathering in underground wireless sensor networks," *Pers. Ubiquitous Comput.*, vol. 2020, pp. 1–18, Sep. 2020.
[13] S. Kisseleff, I. F. Akyildiz, and W. H. Gerstacker, "Digital signal transmission in magnetic induction based wireless underground sensor networks," *IEEE Trans. Commun.*, vol. 63, no. 6, pp. 2300–2311, Jun. 2015.

[14] D. Lin, W. Min, and J. Xu, "An energy-saving routing integrated economic theory with compressive sensing to extend the lifespan of WSNs," *IEEE Internet Things J.*, vol. 7, no. 8, pp. 7636–7647, Aug. 2020.
[15] G. Liu, "A Q-learning-based distributed routing protocol for frequency-switchable magnetic induction-based wireless underground sensor networks," *Future Gener. Comput. Syst.*, vol. 139, pp. 253–266, Feb. 2023.
[16] X. Tan and Z. Sun, "On environment-aware channel estimation for wireless sensor networks using magnetic induction," in *Proc. IEEE Conf. Comput. Commun. Workshops*, 2017, pp. 217–222.
[17] L. Huang, J. Zou, Y. Zhou, Y. Hong, J. Zhang, and Z. Ding, "Effect of vertical metal plate on transfer efficiency of the wireless power transfer system," *Energies*, vol. 12, no. 19, Oct. 2019, Art. no. 3790.
[18] N. Saeed, M.-S. Alouini, and T. Y. Al-Naffouri, "Toward the Internet of Underground Things: A systematic survey," *IEEE Commun. Surveys Tuts.*, vol. 21, no. 4, pp. 3443–3466, Oct.–Dec. 2019.
[19] H. T. H. Trang, L. T. Dung, and S. O. Hwang, "Connectivity analysis of underground sensors in wireless underground sensor networks," *Ad Hoc Netw.*, vol. 71, no. 15, pp. 104–116, Mar. 2018.
[20] A. V. Goldberg, "Efficient graph algorithms for sequential and parallel computers," Ph.D. thesis, Massachusetts Inst. Technol., Cambridge, MA, USA, 1987.
[21] A. Goldberg and R. Tarjan, "A new approach to the maximum-flow problem," *J. ACM*, vol. 35, no. 4, pp. 921–940, Oct. 1988.
[22] G. Borradaile, P. N. Klein, S. Mozes, Y. Nussbaum, and C. Wulff-Nilsen, "Multiple-source multiple-sink maximum flow in directed planar graphs in near-linear time," *SIAM J. Comput.*, vol. 46, no. 4, pp. 1280–1303, Apr. 2017.
[23] D. O. M. Tuller and D. Hillel, "Retention of water in soil and the soil water characteristic curve," *Encyclopedia Soils Environ.*, vol. 4, pp. 278–289, Apr. 2004.

Guanghua Liu (Member, IEEE) received the Ph.D. degree in information and communication engineering from the Huazhong University of Science and Technology, Wuhan, China, in 2019.

He is currently an Associate Professor with the Research Center of 6G Mobile Communications, School of Cyber Science and Engineering, Huazhong University of Science and Technology. From 2017 to 2019, he was with the State University of New York at Buffalo, Amherst, NY, USA. He has authored or coauthored many papers published in *IEEE Communications Magazine*, IEEE TRANSACTIONS ON COMMUNICATIONS, and other international top journals. His research interests include wireless underground/underwater communications, millimeter-wave detection, wireless power transfer, Internet of Things, and wireless weak-link sensor network security.

Dr. Liu was the recipient of the First Prize of Science and Technology Progress of Chinese Society of Electronics in 2021. He is an External Expert of ERC Starting Grant, a Member of CIC Professional Committee on Antennas and RF Technology, an Editorial Board Member of international journals, such as *China Communications,* and a TPC member of a series of international conferences, such as WWW-2024, Chinacom-2015, and so on. He is a Reviewer for IEEE TRANSACTIONS ON VEHICULAR TECHNOLOGY, IEEE TRANSACTIONS ON COMMUNICATIONS, IEEE TRANSACTIONS ON WIRELESS COMMUNICATIONS, and *IEEE Communications Magazine*.